TOR complex 2–regulated protein kinase Ypk1 controls sterol distribution by inhibiting StARkin domain–containing proteins located at plasma membrane–endoplasmic reticulum contact sites

Françoise M. Roelants[a], Neha Chauhan[b], Alexander Muir[a,†], Jameson C. Davis[a], Anant K. Menon[b], Timothy P. Levine[c], and Jeremy Thorner[a,*]

[a]Department of Molecular and Cell Biology, University of California, Berkeley, Berkeley, CA 94720-3202; [b]Department of Biochemistry, Weill Cornell Medical College, New York, NY 10065; [c]UCL Institute of Ophthalmology, University College London, London EC1V 9EL, UK

ABSTRACT **In our proteome-wide screen, Ysp2 (also known as Lam2/Ltc4) was identified as a likely physiologically relevant target of the TOR complex 2 (TORC2)–dependent protein kinase Ypk1 in the yeast *Saccharomyces cerevisiae*. Ysp2 was subsequently shown to be one of a new family of sterol-binding proteins located at plasma membrane (PM)–endoplasmic reticulum (ER) contact sites. Here we document that Ysp2 and its paralogue Lam4/Ltc3 are authentic Ypk1 substrates in vivo and show using genetic and biochemical criteria that Ypk1-mediated phosphorylation inhibits the ability of these proteins to promote retrograde transport of sterols from the PM to the ER. Furthermore, we provide evidence that a change in PM sterol homeostasis promotes cell survival under membrane-perturbing conditions known to activate TORC2-Ypk1 signaling. These observations define the underlying molecular basis of a new regulatory mechanism for cellular response to plasma membrane stress.**

Monitoring Editor
John York
Vanderbilt University

Received: Apr 17, 2018
Revised: Jun 12, 2018
Accepted: Jun 13, 2018

INTRODUCTION

Sterols in the plasma membranes (PMs) of eukaryotic cells (van Meer *et al.*, 2008; Hannich *et al.*, 2011; Klug and Daum, 2014) affect their fluidity and permeability and induce phase separations, including sphingolipid-enriched sterol-containing microdomains that influence the distribution and function of integral membrane proteins (Lingwood and Simons, 2010; Yang *et al.*, 2016). Sterols are synthesized de novo in the endoplasmic reticulum (ER) and delivered to the membranes of other organelles, in part, by nonvesicular mechanisms requiring lipid transfer proteins (LTPs; Raychaudhuri and Prinz, 2010; Chiapparino *et al.*, 2016; Drin *et al.*, 2016; Kentala *et al.*, 2016; Dittman and Menon, 2017). One class of sterol-specific LTPs are members of the family of steroidogenic acute regulatory transfer (StART) proteins (Tsujishita and Hurley, 2000; Lavigne *et al.*, 2010; Maxfield *et al.*, 2016). Recently, a new family of ER membrane–anchored StART-like (also called StARkin) domain-containing proteins were discovered that are conserved from yeast (*Saccharomyces cerevisiae*) to humans and located at ER–PM, ER–mitochondria, and ER–vacuole junctions (Gatta *et al.*, 2015; Murley *et al.*, 2015; Wong and Levine, 2016). How this novel class of sterol-binding StARkin domain-containing proteins is regulated is poorly understood.

In yeast, the TORC2-activated protein kinase Ypk1 (and its paralogue Ypk2) is an essential regulator of PM sphingolipid, glycerolipid, and protein homeostasis (Roelants *et al.*, 2010, 2011, 2017; Lee *et al.*, 2012; Muir *et al.*, 2014, 2015; Alvaro *et al.*, 2016). A systematic screen to pinpoint presumptive substrates of Ypk1 identified Ysp2/Lam2/Ltc4 (Muir *et al.*, 2014), one member of the new family of StART-like domain-containing proteins (Gatta *et al.*, 2015; Murley *et al.*, 2015). Contrary to a prior claim that it is a mitochondrial protein (Sokolov *et al.*, 2006), Ysp2 and its paralogue Lam4/Ltc3 are located

This article was published online ahead of print in MBoC in Press (http://www.molbiolcell.org/cgi/doi/10.1091/mbc.E18-04-0229) on June 21, 2018.

†Present address: Vander Heiden Lab, Department of Biology and Koch Institute for Integrative Cancer Research, Massachusetts Institute of Technology, Cambridge, MA 02139.

*Address correspondence to: Jeremy Thorner (jthorner@berkeley.edu).

Abbreviations used: 3MB-PP1, 1-(*tert*-butyl)-3-(3-methylbenzyl)-1H-pyrazolo[3,4-d]pyrimidin-4-amine; ACAT, acyl-CoA:sterol acyltransferase; AmB, amphotericin B; ER, endoplasmic reticulum; GRAM, PH-like domain recognized first in glucosyltransferases, Rab GTPase activators, and myotubularins; HMG-CoA, hydroxymethylglutaryl-coenzyme A; LTP, lipid transfer protein; PH, pleckstrin homology; PM, plasma membrane; SCD, synthetic complete medium containing dextrose/glucose as the carbon source; StART, steroidogenic acute regulatory transfer; StARkin, StART-related sterol-binding domain; TOR, target-of-rapamycin (protein kinase catalytic subunit); TORC2, TOR complex 2; WT, wild type.

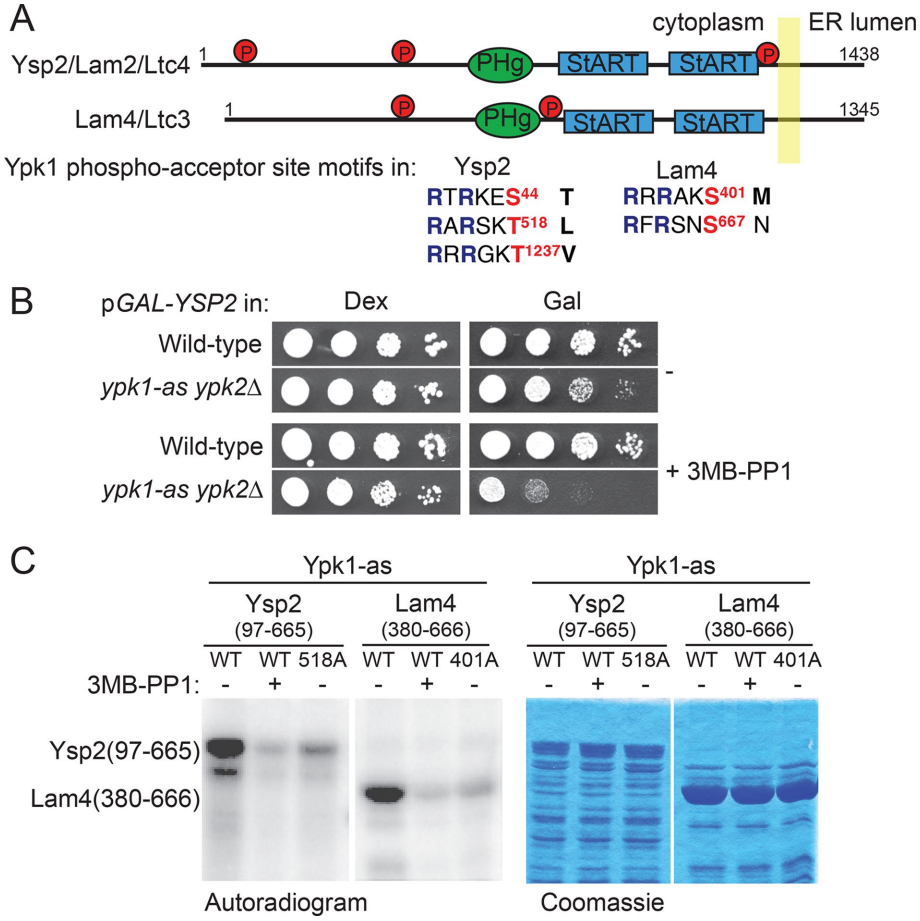

FIGURE 1: Ypk1 phosphorylates Ysp2 at T518 and Lam4 at S401. (A) Diagram of the Ysp2/Lam2/Ltc4 and Lam4/Ltc3 proteins showing the localization of the Ypk1 phosphoacceptor site motifs RxRxxS/TΦ (where Φ is any hydrophobic amino acid) in red. Also shown are the PH-like (GRAM) domain in green and the StART domains 1 and 2 in blue, as well as the predicted transmembrane domain in yellow. (B) Serial 10-fold dilutions of wild-type (BY4741) or *ypk1-as ypk2*Δ (yAM135-A) cells transformed with p*GAL-YSP2* (pAX177) were spotted on plates with dextrose (no protein expression) or galactose (to induce protein expression) in the absence (–) or presence of 1 μM 3MB-PP1. The plates were scanned after incubation for 3 d at 30°C. (C) GST-Ysp2(97-665) (pAX228), GST-Ysp2(97-665)^{T518A} (pJD6), GST-Lam4(380-666) (pJD4), and GST-Lam4(380-666)^{S401A} (pJD5) were purified from *E. coli* and incubated with [γ-^{32}P]ATP and *ypk1-as*, purified from *S. cerevisiae*, in the absence or presence of 3MB-PP1. The products were then resolved by SDS–PAGE and analyzed.

at ER-PM contact sites and are involved in retrograde transfer of exogenously supplied sterols from the PM to the ER (Gatta *et al.*, 2015; Murley *et al.*, 2015). The StART-like domains isolated from these proteins bind ergosterol and are able to transfer sterols between vesicles in vitro (Gatta *et al.*, 2015; Murley *et al.*, 2015; Horenkamp *et al.*, 2018; Jentsch *et al.*, 2018; Tong *et al.*, 2018). Here we confirmed, first, that Ysp2 is an authentic target of Ypk1-mediated phosphorylation. We then investigated whether this modification affects sterol transfer between the PM and the ER. Finally, we examined whether this regulation is important in sustaining cell viability under stressful conditions (namely, sphingolipid depletion and high exogenous acetic acid) that are known to activate TORC2-Ypk1 signaling (Roelants *et al.*, 2011; Berchtold *et al.*, 2012; Guerreiro *et al.*, 2016).

RESULTS

Ypk1 phosphorylates Ysp2 and Lam4

Ysp2 has three consensus Ypk1 phosphorylation sites [-**R**-x-**R**-x-x-**S**/**T**-(Hpo)-, where (Hpo) indicates a preference for a hydrophobic residue] and its paralogue Lam4 has two (Figure 1A), with T518 in Ysp2 located at a relative position similar to that of S401 in Lam4. We have shown before that one hallmark of authentic Ypk1 substrates is that their overexpression is inhibitory to growth when Ypk1 function is limiting (Muir *et al.*, 2014). Indeed, in *ypk1-as ypk2*Δ cells, which contain an allele of Ypk1 sensitive to inhibition by the adenine analog 3MB-PP1, *GAL* promoter–driven overexpression of Ysp2 prevented growth more potently in the presence of inhibitor than in its absence, but had no effect on otherwise wild-type (WT) cells with or without inhibitor (Figure 1B). In vitro, purified Ypk1-as phosphorylated both a fragment of Ysp2 containing its T518 site (GST-Ysp2(97-665)) and a fragment of Lam4 containing its S401 site (GST-Lam4(380-666)) in the absence of 3MB-PP1, but not in its presence, and mutation of each of these two residues to Ala confirmed that the observed incorporation was occurring mainly at the expected sites (Figure 1C). We then focused on examining Ysp2 phosphorylation in vivo because a *ysp2*Δ single mutant exhibits a readily detectable defect in retrograde transport of exogenously supplied sterol compared with WT cells, whereas a *lam4*Δ single mutant does not (Gatta *et al.*, 2015). We analyzed the migration pattern of a FLAG-tagged derivative of a C-terminal fragment of Ysp2 [Ysp2(499-1438)] containing two (T518 and T1237) of its three Ypk1 sites using phosphate affinity (Phos-tag) gel electrophoresis (Kinoshita *et al.*, 2015). Treatment with the sphingolipid biosynthesis inhibitor myriocin, a stress that markedly stimulates TORC2-mediated activation of Ypk1 (Roelants *et al.*, 2011; Berchtold *et al.*, 2012), greatly increased the less mobile (more highly phosphorylated) species and concomitantly reduced the fastest (hypophosphorylated) species, and this myriocin-evoked mobility shift was largely eliminated by mutation of the two Ypk1 sites to Ala (Figure 2A), by phosphatase treatment (Figure 2B), or in *ypk1-as ypk2*Δ cells treated with 3MB-PP1 (Figure 2C). Thus, Ysp2 is phosphorylated at its Ypk1 sites in vivo and in a manner reflecting the state of Ypk1 activation.

Ypk1 phosphorylation inhibits Ysp2 function

Comparison of WT Ysp2 with a mutant (Ysp2^{AAA}) lacking all three of the Ypk1 consensus phosphoacceptor sites demonstrated that neither the steady-state level (Figure 3A) nor the localization (Figure 3B) of Ysp2 is affected by the lack of Ypk1-mediated phosphorylation. As a first means to examine whether Ypk1 phosphorylation affects Ysp2 function, we took advantage of the fact that killing by the antibiotic amphotericin B (AmB) results from its specific interaction with ergosterol in the PM of fungal cells, disrupting the permeability barrier (Kamiński, 2014). Cells lacking Ysp2 are more sensitive to AmB than WT cells (Gatta *et al.*, 2015), indicating an increase in the pool of ergosterol that is accessible to AmB. Indeed, at the concentration

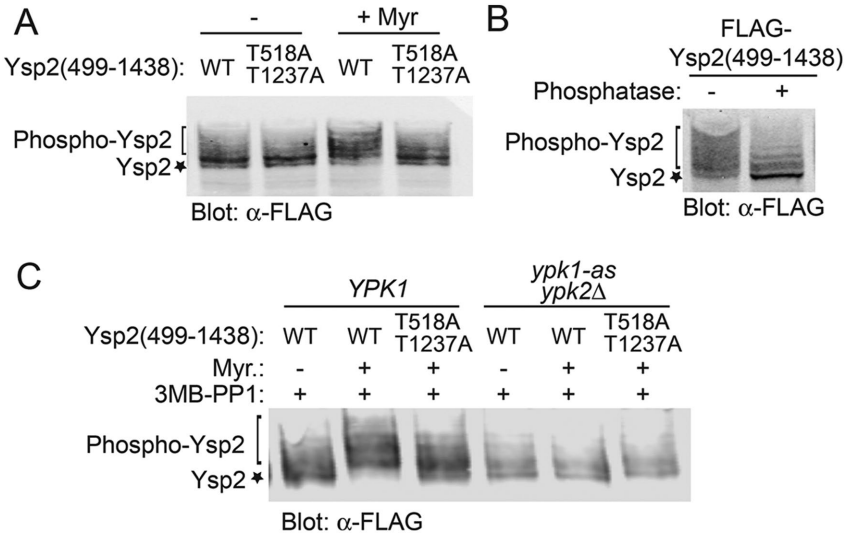

FIGURE 2: Ysp2 is phosphorylated in a Ypk1-dependent manner in vivo. (A) Wild-type (BY4741) cells expressing either 3xFLAG-Ysp2(499-1438) (pFR355) or 3xFLAG-Ysp2^{AA}(499-1438) (pFR357) from the *GAL1* promoter were grown to mid–exponential phase, induced with galactose for 1 h, and then treated with vehicle (–) or 1.25 μM myriocin for 2 h, after which extracts were prepared, resolved on a Phos-tag SDS–PAGE (35 μM Phos-tag), and analyzed by immunoblotting. (B) Extracts of wild-type (BY4741) cells expressing 3xFLAG-Ysp2(499-1438) (pFR355) were treated with phosphatase, resolved on a Phos-tag SDS–PAGE (35 μM Phos-tag), and analyzed by immunoblotting. (C) The same cells as in A, as well as *ypk1-as ypk2*Δ (YAM135-A) cells expressing either 3xFLAG-Ysp2(499-1438) (pFR355) or 3xFLAG-Ysp2^{AA}(499-1438) (pFR357), were grown to mid–exponential phase, induced with galactose for 1 h, and then treated with 10 μM 3MB-PP1 and vehicle (–) or 1.25 μM myriocin for 2 h and analyzed as in A.

of AmB we used, *ysp2*Δ cells carrying vector alone were unable to grow, whereas expression of WT Ysp2 from the same vector exhibited detectable growth (Figure 4A). Strikingly, expression of either Ysp2^{T518A} or Ysp2^{AAA} from the same vector conferred a level of AmB resistance reproducibly higher than that of WT Ysp2 and markedly greater than in *ysp2*Δ cells (Figure 4A), indicating that cells expressing Ysp2^{T518A} and Ysp2^{AAA} have even less accessible ergosterol in their PM than WT cells. This difference is due to a modification in the distribution of ergosterol rather than in the level of cellular ergosterol, as Ysp2^{AAA} and WT Ysp2 cells contain the same amount of total ergosterol (Figure 4B). The change in PM ergosterol homeostasis was confirmed by showing that cells expressing Ysp2^{AAA} are more resistant than cells expressing WT Ysp2 to nystatin, another pore-forming polyene antifungal that functions, in part, by interacting with ergosterol in membranes (Dos Santos *et al.,* 2017; Figure 4C). Therefore, the role of Ypk1 phosphorylation is to negatively regulate Ysp2 function. Examination of other single mutants (Ysp2^{S44A} and Ysp2^{T1237A}) indicated that the primary inhibitory site is T518 (Figure 4A). We also tested cells expressing Ysp2^{T518E} and Ysp2^{EEE} mutants to determine whether they might resemble permanently phosphorylated Yps2 and thus be more sensitive to AmB than cells expressing WT Yps2, but this was not the case (Supplemental Figure 1, A and B), indicating that, in this protein, an acidic residue(s) does not mimic its authentic phosphorylation.

Given the importance of T518 in Ysp2 for its negative regulation by Ypk1, and the similar location of S401 in Lam4, we also tested the AmB sensitivity of WT Lam4 and a Lam4^{S401A} mutant. At the concentration of AmB used, *ysp2*Δ *lam4*Δ double mutant cells carrying vector alone were unable to grow (cells lacking both Lam4 and Ysp2 are more sensitive to AmB than those lacking Ysp2 alone [Supplemental Figure 2]), whereas expression of WT Ysp2 from the same vector restored readily detectable growth and expression of Ysp2^{T518A} conferred a markedly higher level of AmB resistance, as expected (Figure 4D). Expression of WT Lam4 from the same vector restored only a very modest degree of growth, but, revealingly, expression of Lam4^{S410A} reproducibly conferred a higher degree of AmB resistance. The observed phenotype of Lam4^{S401A} (Figure 4D) indicates that phosphorylation by Ypk1 also negatively regulates Lam4.

Ysp2 promotes the retrograde transport of exogenously supplied sterols from the PM to the ER, detected by measuring conversion of sterols to steryl esters by the ER-localized acyltransferases Are1 and Are2 (Figure 5A; Gatta *et al.,* 2015). Therefore, as a second and independent way to assess the functional consequences of Ypk1 phosphorylation for Ysp2, we analyzed the rate of uptake and esterification of two different reporter sterols, [^{3}H]cholesterol and fluorescent dehydroergosterol (DHE), using methods described previously (Georgiev *et al.,* 2011; Gatta *et al.,* 2015; Figure 5A). Both cholesterol esters and DHE esters were accumulated faster (by ≥30% and

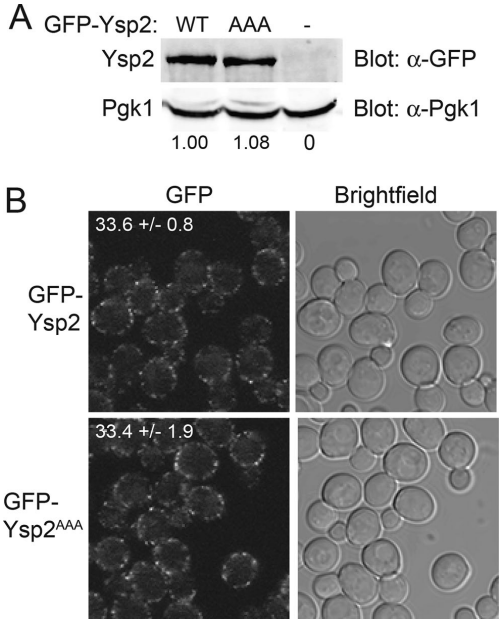

FIGURE 3: Phosphorylation at the Ypk1 sites does not affect levels or localization of Ysp2. (A) Extracts from cultures of *ysp2*Δ (YFR484) cells carrying pRS416 (empty vector) or expressing from the same vector GFP-Ysp2 or GFP-Ysp2^{AAA} (pFR332) were prepared, resolved by SDS–PAGE, and analyzed by immunoblotting. (B) Strains GFP-Ysp2 (YFR512) and GFP-Ysp2^{AAA} (YFR511) were grown to mid–exponential phase and viewed with fluorescence microscopy. The numbers indicate the fluorescence (a.u.) per area of cell in sets of three images (400–500 cells per image).

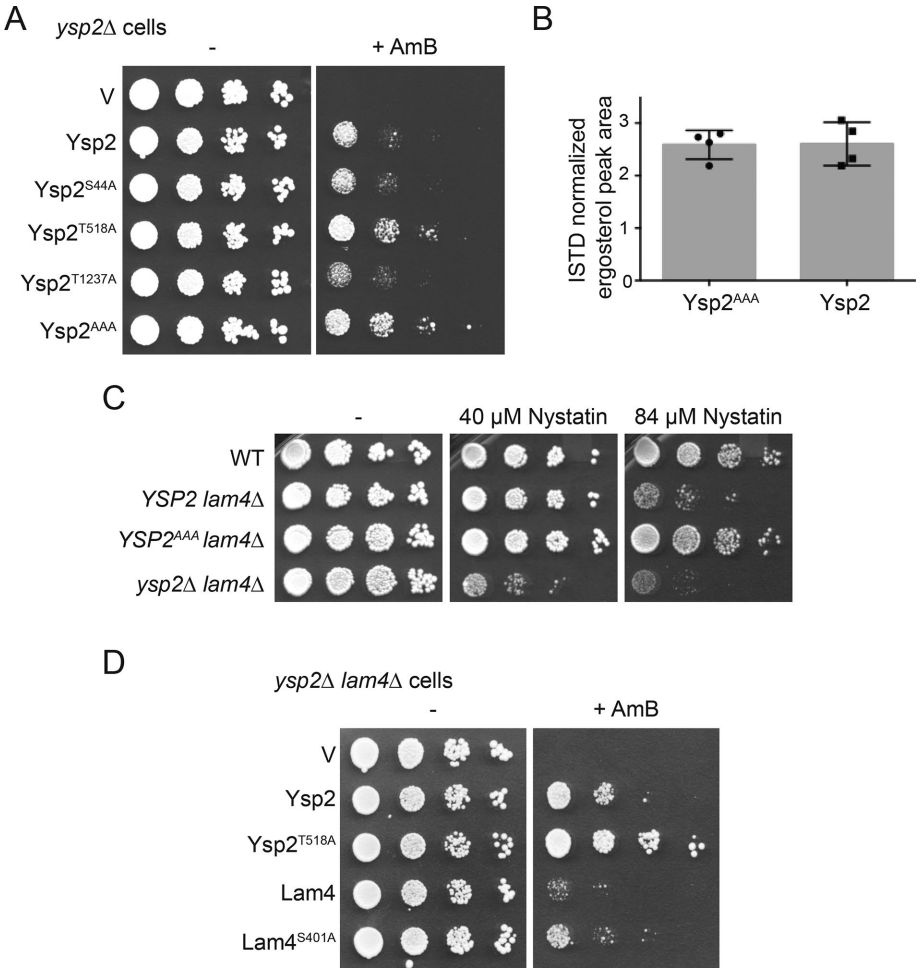

FIGURE 4: Phosphorylation at the Ypk1 sites down-regulates the activity of Ysp2. (A) Serial 10-fold dilutions of *ysp2*Δ (YFR484) cells carrying pRS416 (empty vector) or expressing from the same vector GFP-Ysp2, GFP-Ysp2^{S44A} (pFR333), GFP-Ysp2^{T518A} (pFR325), GFP-Ysp2^{T1237A} (pFR340), or GFP-Ysp2^{AAA} (pFR332) were spotted on plates lacking (–) or containing AmB (0.16 μM). The plates were scanned after incubation for 2 d at 30°C. (B) Total ergosterol levels of Ysp2^{AAA} (YFR494-A) and Ysp2^{WT} (YFR495) cells was quantified as described in *Materials and Methods*. Four samples of each strain were counted in triplicate. (C) Serial 10-fold dilutions of WT (BY4741) or otherwise isogenic *lam4*Δ (YFR516), Ysp2^{AAA}*lam4*Δ (YFR514), and *ysp2*Δ *lam4*Δ (YFR513) cells were spotted on plates lacking (–) or containing nystatin at the indicated concentrations. The plates were scanned after incubation for 3 d at 30°C. (D) As in A except that *ysp2*Δ *lam4*Δ (YFR513) cells carrying pRS416 (empty vector) or expressing from the same vector GFP-Ysp2, GFP-Ysp2^{T518A} (pFR325), GFP-Lam4, or GFP-Lam4^{S401A} (pFR358) were used and the plates were scanned after incubation for 3 d at 30°C.

≥45%, respectively) in cells expressing Ysp2^{AAA} than in cells expressing WT Ysp2 (Figure 5, B and C), indicating that Ysp2 is more active when it is not phosphorylated by Ypk1. The increased rate of DHE ester accumulation was not attributable to any difference in the efficiency of initial DHE loading in the PM (Figure 5D) nor to any difference in activity of the ACAT enzymes Are1 and Are2 in cells expressing Ysp2^{AAA} compared with cells expressing WT Ysp2 (Figure 5E). Thus, these direct biochemical assays confirmed that Ypk1 phosphorylation negatively regulates the ability of Ysp2 to mediate transport of sterols from the PM to the ER.

A change in ergosterol homeostasis helps compensate for the PM stress of sphingolipid depletion

Our findings predict that activation of TORC2-Ypk1 signaling in response to the sphingolipid depletion caused by myriocin treatment would increase sensitivity to AmB because Ypk1-mediated phosphorylation of both Ysp2 and Lam4 would result in more accessible ergosterol in the PM and, further, that this hypersensitivity should be alleviated in the Ysp2^{AAA} mutant (Figure 6A). To focus on Ysp2, because it seems to have the major influence on sterol influx (Gatta *et al.*, 2015), we tested these predictions in *lam4*Δ cells. In agreement with our hypothesis, we found, first, that a concentration of AmB that is sublethal to cells expressing WT Ysp2 in the absence of myriocin treatment was able to kill cells treated with a concentration of myriocin that, by itself, was insufficient to compromise cell viability (Figure 6B). Second, cells expressing Ysp2^{AAA} were indeed more resistant to AmB in the presence of myriocin than cells expressing WT Ysp2 (Figure 6B). Thus, when activated by myriocin treatment, Ypk1-mediated phosphorylation of Ysp2 leads to an increase of accessible PM ergosterol, enhancing sensitivity to AmB.

The change in ergosterol homeostasis at the PM appears to be important for counteracting a reduction in sphingolipid content, because cells expressing Ysp2^{AAA}, which have less accessible ergosterol in the PM and are more resistant to AmB than cells expressing WT Ysp2 (Figure 6C), are, conversely, more sensitive to myriocin than WT cells (Figure 6D). Consistent with this view, *ysp2*Δ cells, which are very sensitive to killing by AmB (Figure 6C), are more resistant to myriocin than WT cells (Figure 6D). Collectively, these results indicate that, upon sphingolipid limitation, activated Ypk1 phosphorylates and impedes Ysp2-mediated ergosterol transport, resulting in enhanced survival under this stressful condition (Figure 6, A and D).

As a second and independent way to determine whether activation of TORC2-Ypk1 signaling increases sensitivity to AmB because Ypk1-mediated phosphorylation inhibits Ysp2 and Lam4, cells were grown in medium containing acetic acid, another condition that has been shown to activate the TORC2-Ypk1 pathway (Guerreiro *et al.*, 2016). Again, in agreement with our hypothesis, a concentration of AmB that is sublethal to cells expressing WT Ysp2 in the absence of acetic acid treatment was able to kill cells treated with a concentration of acetic acid that, by itself, was insufficient to compromise cell viability (Figure 6E) and cells expressing Ysp2^{AAA} were more resistant to AmB in the presence of acetic acid than cells expressing WT Ysp2 (Figure 6E). Interestingly, control of ergosterol in the PM appears to contribute to acetic acid toxicity, as cells expressing Ysp2^{AAA}, which have less accessible ergosterol in the PM, are more resistant to acetic acid than cells expressing WT Ysp2, whereas *ysp2*Δ cells are much more sensitive than WT cells (Figure 6F).

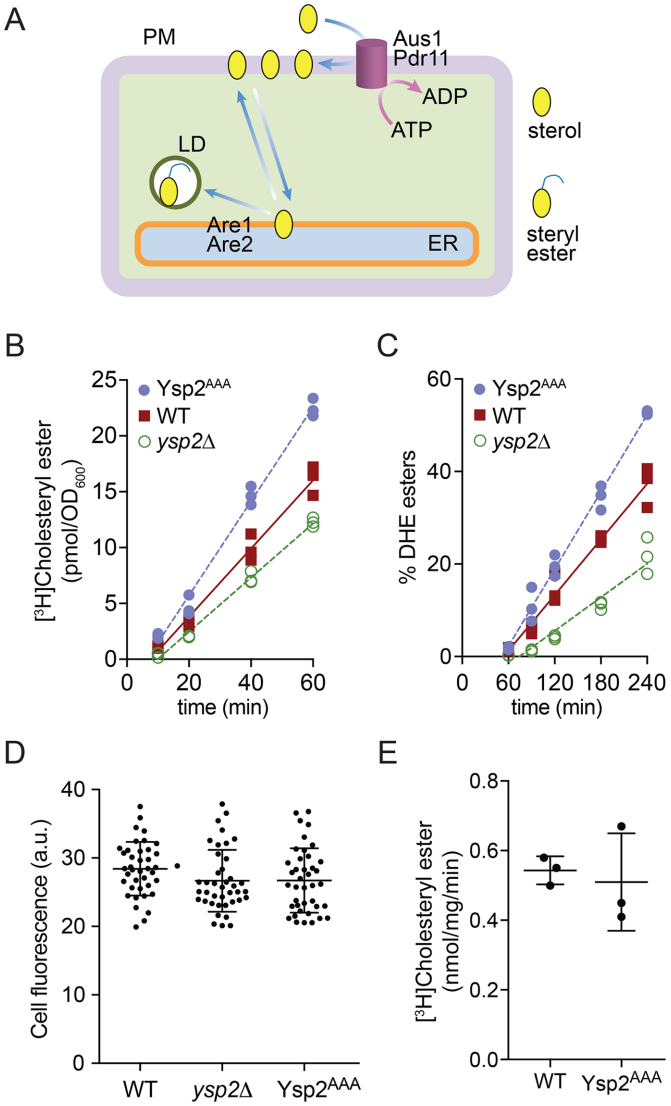

FIGURE 5: Retrograde transfer of sterols is slower when Ysp2 is phosphorylated by Ypk1. (A) Depiction of the assay. (B) Retrograde traffic of [^{3}H]cholesterol was determined for strains *upc2-1* Ysp2 (YFR509), *upc2-1 ysp2*Δ, and *upc2-1* Ysp2^{AAA} (YFR510) as described in *Materials and Methods*. Mutation in the Upc2 transcription factor is necessary to allow cholesterol uptake. SEM was calculated from the scores of at least three independent experiments ($p < 0.035$). (C) Wild-type (YFR495), *ysp2*Δ (YFR484), and Ysp2^{AAA} (YFR494) strains were incubated with DHE under hypoxic conditions to enable the fluorescent sterol to enter the PM (hypoxic incubation overcomes "aerobic sterol exclusion" and is required for DHE loading). After cells were chased under aerobic conditions, lipids were extracted from the cells at the indicated time points and the percentage of DHE that was converted to DHE ester was determined. SEM was calculated from the scores of at least four independent experiments ($p < 0.0024$). (D) Loading of DHE in the PM of WT Ysp2 (YFR495) and Ysp2^{AAA} (YFR494) cells was determined as described in *Materials and Methods*. (E) ACAT (Acyl-CoA:sterol acyltransferase) activity was assayed in vitro for WT Ysp2 (YFR495) and Ysp2^{AAA} (YFR494) cells, as described in *Materials and Methods*.

DISCUSSION

As documented here, a reduction in sphingolipid levels sensitizes yeast cells to the action of AmB (Figure 6B). Our findings are in agreement with a study that showed that perturbing sphingolipid production (by null mutations in genes encoding enzymes [Elo2/Fen1 and Elo3/Sur4] involved in synthesis of the very-long-chain fatty acid [C26] that is normally incorporated into yeast ceramides) caused both *S. cerevisiae* and *Candida albicans* to be two to five times more sensitive to AmB than control cells (Sharma *et al.*, 2014). As described here, we found that this effect is due, in significant part, to TORC2-activated Ypk1-mediated phosphorylation and inhibition of Ysp2, leaving more accessible ergosterol in the PM.

Other mechanisms likely also contribute to explaining how a reduction in sphingolipids enhances AmB sensitivity. It has been proposed, for example, that sequestration of ergosterol in sphingolipid-enriched microdomains shields it from AmB (Li and Prinz, 2004) and from filipin, another sterol-binding polyene macrolide antibiotic (Jin *et al.*, 2008). An "unshielding" model might explain why *ypk1*Δ cells are more sensitive to AmB than WT cells (Bari *et al.*, 2015). First, *ypk1*Δ cells have dysregulated transbilayer lipid asymmetry (Roelants *et al.*, 2010). Second, overall sphingolipid levels are lower in *ypk1*Δ mutants than in control cells (da Silveira Dos Santos *et al.*, 2014) because Ypk1 action stimulates sphingolipid biosynthesis both at its first committed step (Roelants *et al.*, 2011) and at the level of ceramide synthase (Muir *et al.*, 2014).

Our studies have uncovered a TORC2- and Ypk1-dependent mechanism by which sphingolipid levels regulate PM sterol. Could the opposite be true too? Yeast strains lacking Ypk1 are sensitive to fluconazole, an inhibitor of ergosterol biosynthesis (Gupta *et al.*, 2003; Hillenmeyer *et al.*, 2008), and synthesis of certain sphingolipids is up-regulated upon sterol depletion in *Drosophila* (Carvalho *et al.*, 2010). However, in marked contrast to its activation upon sphingolipid depletion (Roelants *et al.*, 2011; Berchtold *et al.*, 2012), TORC2 was not activated when sterol synthesis was blocked by treatment with lovastatin (Supplemental Figure 3). Lovastatin, a potent inhibitor of HMG-CoA reductase, a key enzyme in the mevalonate pathway, blocks isoprenoid and sterol synthesis in yeast (Basson *et al.*, 1986; Hampton and Rine, 1994; Kuranda *et al.*, 2010). Thus, TORC2 does not serve as a sensor of sterol depletion. However, a recent study reported a modest elevation in TORC2-Ypk1 activity in *ysp2*Δ *lam4*Δ cells, suggesting that an increase in PM ergosterol availability somehow enhances TORC2 function (Murley *et al.*, 2017). On the basis of a proteome-wide lipidomics screen, it was reported that Ypk1 binds ergosterol and further that ergosterol is required for Ypk1 activity (Li *et al.*, 2010), and thus that Ypk1 itself might serve as a sterol sensor. However, subsequent work documented that ergosterol is not required for either basal or myriocin-induced Ypk1 function (Roelants *et al.*, 2011). Moreover, if ergosterol were an essential Ypk1 activator, lack of ergosterol would decrease Ypk1 activity, with a concomitant drop in sphingolipids, which would be deleterious to PM integrity.

Important questions remain about how Ysp2 participates in transfer of sterol from the PM to the ER and how its phosphorylation by Ypk1 impedes that function. Determining whether phosphorylation affects the sterol binding and/or transfer properties of Ysp2, its interaction with other lipids in the PM, or its association with other proteins present at ER-PM contact sites is an essential next step to investigate. In any event, here we have uncovered the mechanism of a previously uncharacterized and physiologically important level of regulation. Moreover, we have documented here that, under conditions that cause PM stress (especially limiting the rate of sphingolipid production), activation of TORC2-Ypk1 signaling and the ensuing inhibition of Ysp2 allows cells to compensate by apparently retarding removal of

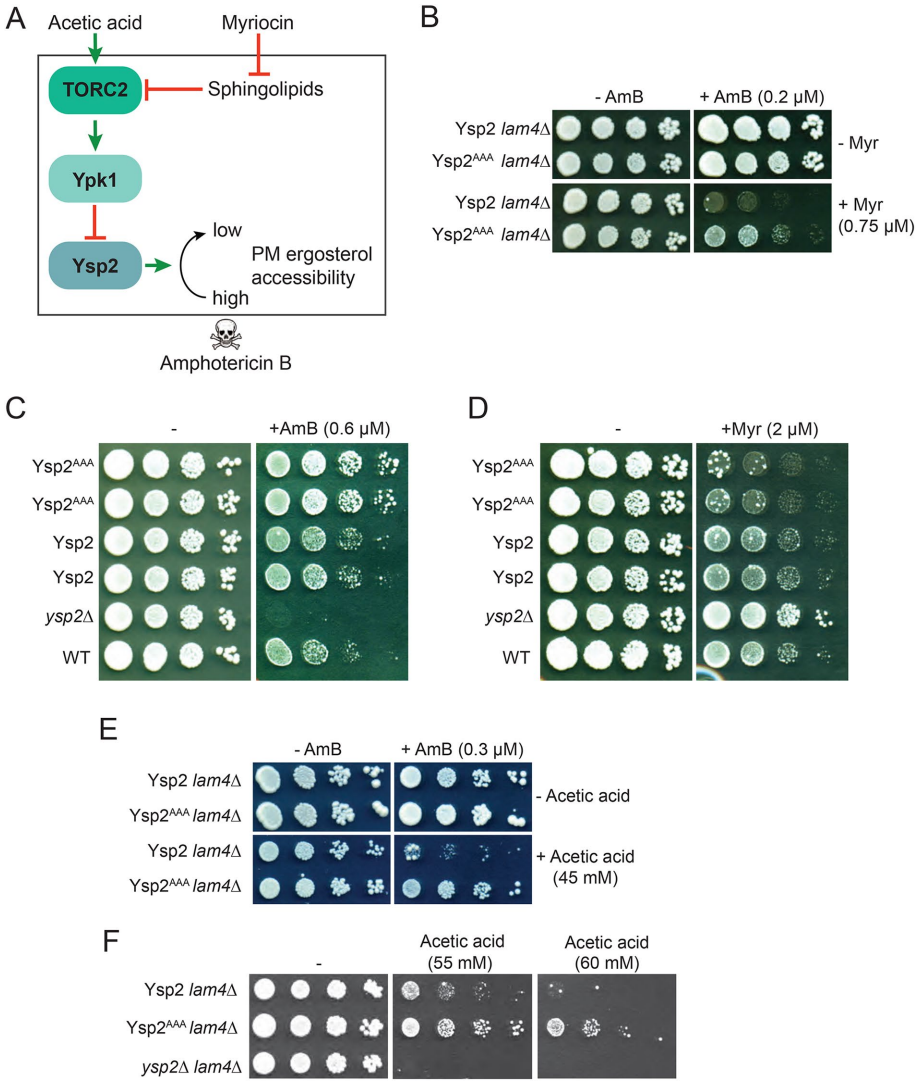

FIGURE 6: Reorganizing ergosterol in the PM helps compensate when sphingolipids are limiting and reduces resistance to acetic acid. (A) Schematic depiction of TORC2-Ypk1 control of PM ergosterol level. (B) Serial 10-fold dilutions of Ysp2^{WT}*lam4*Δ (YFR516) and Ysp2^{AAA}*lam4*Δ (YFR514) cells were spotted on plates lacking (–) or containing 0.2 μM AmB minus or plus 0.75 μM Myr. The plates were scanned after incubation for 3 d at 30°C. (C) Serial 10-fold dilutions of Ysp2^{AAA} (YFR494-A and YFR494-B) or Ysp2^{WT} (YFR495-A and YFR495-B), *ysp2*Δ, and BY4741 cells were spotted on plates lacking (–) or containing AmB at the indicated concentrations. The plates were scanned after incubation for 3 d at 30°C. (D) The same cells as in C were spotted on plates lacking or containing myriocin (Myr) at the indicated concentration. (E) The same cells as in B were grown to stationary phase in synthetic complete (SC) medium containing glucose/dextrose (D) as the carbon source at pH 4; then serial 10-fold dilutions were made and spotted onto SCD plates lacking (–) or containing 0.3 μM AmB minus or plus 45 mM acetic acid. The plates were scanned after incubation for 4 d at 30°C. (F) Serial 10-fold dilutions of *lam4*Δ (YFR516), Ysp2^{AAA}*lam4*Δ (YFR514), and *ysp2*Δ *lam4*Δ (YFR513) cells grown as in E were spotted onto plates lacking (–) or containing acetic acid at the indicated concentrations. The plates were scanned after incubation for 3 d at 30°C.

ergosterol from the PM. Given that Ypk1 has already been shown to control sphingolipid synthesis (Roelants *et al.*, 2011; Muir *et al.*, 2014), glycerolipid synthesis (Lee *et al.*, 2012; Muir *et al.*, 2015), and leaflet distribution (Roelants *et al.*, 2010), as well as the rate of endocytosis of integral plasma membrane proteins (Rispal *et al.*, 2015; Alvaro *et al.*, 2016; Roelants *et al.*, 2017), our current findings add sterols to the list of PM components under the control of Ypk1 action.

MATERIALS AND METHODS

Strains and growth conditions

Yeast strains used in this study (Table 1) were grown routinely at 30°C. Standard rich (YP) and defined minimal (SC) media (Sherman *et al.*, 1986) containing either 2% glucose (Glc), 2% raffinose and 0.2% sucrose (Raf-Suc), or 2% galactose (Gal) as the carbon source, as indicated, and supplemented with appropriate nutrients to maintain selection for plasmids, were used for yeast cultivation. For gene induction from the *GAL1* promoter, cells were pregrown to mid–exponential phase in SC + Raf-Suc medium, Gal was added (2% final concentration), and incubation was continued for 3 h. When cells were treated with myriocin (Sigma-Aldrich, St. Louis, MO), the cultures were grown to mid–exponential phase and induced with Gal for 1 h, Myr was added at the final concentration of 1.25 μM, and incubation was continued for an additional 2 h. Standard yeast genetic techniques were performed according to (Sherman *et al.*, 1986).

Plasmids and recombinant DNA methods

Plasmids used in this study (Table 2) were constructed using standard procedures (Sambrook *et al.*, 1989) in *Escherichia coli* strain DH5α. Fidelity of all constructs was verified by nucleotide sequence analysis. All PCRs were performed using Phusion DNA polymerase (ThermoFisher Scientific, Waltham, MA). Site-directed mutagenesis using appropriate mismatch oligonucleotide primers was conducted using the QuickChange method.

Preparation of cell extracts and immunoblotting

The cells in samples (1.5 ml) of an exponentially growing culture ($A_{600\ nm}$ = 0.6) were collected by brief centrifugation, immediately frozen in liquid N_2 and then lysed by resuspension in 150 μl of 1.85 M NaOH, 7.4% β-mercaptoethanol. Protein in the resulting lysate was precipitated by the addition of 150 μl of 50% trichloroacetic acid (TCA) on ice. After 10 min, the resulting denatured protein was collected by centrifugation, washed twice with acetone, and solubilized by resuspension in 80 μl of 0.1 M Tris, 5% SDS, and then 20 μl of a 5X stock of SDS–PAGE sample buffer containing urea was added. After being heated at 39°C for 5 min, portions (3 μl) of the samples containing FLAG-Ysp2(499-1438) were resolved on a Phos-tag gel (8% acrylamide, 35 μM Phos-tag reagent [Wako Pure Chemical Industries, Osaka, Japan]), and samples (10 μl) containing GFP-Ysp2 were resolved by SDS–PAGE (8% acrylamide), transferred to nitrocellulose, incubated with appropriate primary antibodies in Odyssey buffer (Li-Cor Biosciences,

Strain	Genotype	Source/reference
BY4741	*MAT***a** *his3Δ1 leu2Δ0 met15Δ0 ura3Δ0*	Research Genetics
yAM135-A	BY4741 Ypk1(L424A)::*URA3 ypk2*Δ::KanMX4	Muir *et al.*, 2014
YFR484	BY4741 *ysp2*Δ::hphNT1	This study
YFR513	BY4741 *ysp2*Δ::hphNT1 *lam4*Δ::KanMX	This study
YFR495	BY4741 Ysp2::*URA3*	This study
YFR494	BY4741 Ysp2(S44A T518A T1237A)::*URA3*	This study
YFR514	BY4741 Ysp2(S44A T518A T1237A)::*URA3 lam4*Δ::KanMX	This study
YFR512	BY4741 GFP-Ysp2::*URA3*	This study
YFR511	BY4741 GFP-Ysp2(S44A T518A T1237A)::*URA3*	This study
WPY361 (*upc2-1*)	*MAT***a** *upc2-1 ura3-1 his3-11,-15 leu2-3,-112 trp1-1*	Li and Prinz, 2004
*upc2-1 ysp2*Δ	WPY361 *upc2-1 ysp2*Δ	Gatta *et al.*, 2015
YFR509	WPY361 *upc2-1* Ysp2::*URA3*	This study
YFR510	WPY361 *upc2-1* Ysp2(S44A T518A T1237A)::*URA3*	This study
BY4742	*MAT*α *his3Δ1 leu2Δ0 lys2Δ0 ura3Δ0*	Research Genetics
YFR516	BY4742 *lam4*Δ::KanMX *LYS2 met15Δ0*	This study
YFR517	BY4742 Lam4(S401A)::*URA3 LYS2 met15Δ0*	This study
YFR519	BY4742 Ysp2(S44A T518A T1237A)::*URA3* Lam4(S401A)::*URA3 LYS2 met15Δ0*	This study
BJ2168	*MAT***a** *leu2 trp1 ura3-52 prb1-1122 pep4-3 pre1-451 gal2*	Jones, 2002
CGA84	*MAT***a** *leu2Δ1::GEV::NATMX pep4Δ::HIS3 prb1Δ1.6R ura3-52 trp1-1 lys2-801a leu2Δ1 his3Δ200 can1 GAL*	Alvaro *et al.*, 2014

TABLE 1: *S. cerevisiae* strains used in this study.

Lincoln, NE), washed, incubated with appropriate secondary antibodies conjugated to infrared fluorophores, and visualized using an Odyssey infrared imaging system (Li-Cor Biosciences). Antibodies used in this work were 1:10,000 mouse anti-FLAG M2 mAb (Sigma-Aldrich), 1:1,000 mouse anti-GFP mAb (Roche Diagnostics, Indianapolis, IN), 1:10,000 rabbit polyclonal anti-Pgk1 antibodies (Baum *et al.*, 1978); 1:20,000 rabbit polyclonal anti-Ypk1 phospho-T662 antibodies (Niles *et al.*, 2012), and 1:1,000 mouse anti-HA.11 epitope mAb (BioLegend, San Diego, CA).

Protein kinase assay

Ypk1-as was expressed and purified to homogeneity from *S. cerevisiae* as described previously (Muir *et al.*, 2014), incubated at 30°C in protein kinase assay buffer (50 mM Tris-HCl [pH 7.5], 200 mM NaCl, 10 mM $MgCl_2$, 0.1 mM EDTA) with 100 μM [γ-^{32}P] ATP (~5×10^5 cpm/nmol) and 0.5 μg of GST-Ysp2(97-665) or GST-Lam4(380-666) (which were prepared by expression in and purification from *E. coli*, as described below) in the presence or absence of 10 μM 3MB-PP1. After 30 min, reactions were terminated by addition of SDS–PAGE sample buffer containing 6% SDS, followed by boiling for 5 min. Labeled proteins were resolved by SDS–PAGE and analyzed by autoradiography using a PhosphorImager (Molecular Dynamics Division, Amersham Pharmacia Biotech, Piscataway, NJ).

Purification of GST-Ysp2(97-665) and GST-Lam4(380-666) fusion proteins

Freshly transformed BL21(DE3) cells carrying a plasmid expressing the desired GST-fusion protein were grown at 37°C to $A_{600\ nm}$ = 0.6 and expression was induced by addition of isopropyl-β-D-thiogalactopyranoside (0.5 mM final concentration). After vigorous aeration for 4 h at room temperature, cells were harvested and the GST-fusion protein was purified by column chromatography on glutathione-agarose beads using standard procedures.

Fluorescence microscopy

Subcellular localization of GFP-Ysp2 by fluorescence microscopy was conducted as described previously (Gatta *et al.*, 2015).

Yeast growth assays

For cells expressing Ysp2 from the *YSP2* promoter, transformants were cultured overnight in SC media containing 2% dextrose (SCD). Tenfold serial dilutions of overnight cultures starting from $A_{600\ nm}$ = 1.0 were then made in sterile water and spotted onto SCD solid media containing AmB and/or Myr at the indicated concentrations. For cells expressing Ysp2 from the *GAL1* promoter, transformants were cultured overnight in SC media containing 2% raffinose and 0.2% sucrose and the 10-fold serial dilutions were spotted onto SC solid media with 2% galactose (to induce protein expression) or 2% dextrose (no protein expression). These plates also contained 1:1000 dimethyl sulfoxide or 1 μM 3MB-PP1 to inhibit Ypk1-as kinase activity in the *ypk1-as ypk2*Δ strain. Serially spotted cultures were allowed to grow in the dark at 30°C and then scanned on a flatbed scanner.

Sterol import assays

DHE and [^{3}H]cholesterol uptake assays were performed as described previously (Georgiev *et al.*, 2011; Gatta *et al.*, 2015).

ACAT (Acyl-CoA:sterol acyltransferase) activity was assayed in vitro as described in Georgiev *et al.* (2011). ACAT activity was calculated as moles sterol esterified per microgram protein per minute.

Plasmid	Description	Source/reference
pRS416	*CEN*, *URA3*, vector	Sikorski and Hieter, 1989
GFP-Ysp2	pRS416 GFP-Ysp2	Gatta *et al.*, 2015
pFR333	pRS416 GFP-Ysp2(S44A)	This study
pFR325	pRS416 GFP-Ysp2(T518A)	This study
pFR340	pRS416 GFP-Ysp2(T1237A)	This study
pFR332	pRS416 GFP-Ysp2(S44A T518A T1237A)	This study
pFR335	pRS416 GFP-Ysp2(S44E)	This study
pFR331	pRS416 GFP-Ysp2(T518E)	This study
pFR341	pRS416 GFP-Ysp2(T1237E)	This study
pFR343	pRS416 GFP-Ysp2(S44E T518E T1237E)	This study
GFP-Lam4	pRS416 GFP-Lam4	Gatta *et al.*, 2015
pFR358	pRS416 GFP-Lam4(S401A)	This study
YCpLG	*CEN*, *LEU2*, $GAL1_{prom}$ vector	Bardwell *et al.*, 1998
pFR355	YCpLG 3xFLAG-Ysp2(499-1438)	This study
pFR357	YCpLG 3xFLAG-Ysp2(499-1438)(T518A T1237A)	This study
pGEX4T-1	GST tag, bacterial expression vector	GE Healthcare
pJD4	pGEX4T-1 Lam4(380-666)	This study
pJD5	pGEX4T-1 Lam4(380-666)(S401A)	This study
pGEX6P-1	GST tag, bacterial expression vector	GE Healthcare.
pAX228	pGEX6P-1 Ysp2(97-665)	This study
pJD6	pGEX6P-1 Ysp2(97-665)(T518A)	This study
pPL215	pRS416 $MET25_{prom}$-Ypk1-3xHA	Niles *et al.*, 2012
pPL534	pRS416 $MET25_{prom}$-Ypk1(S644A T662A)-3xHA	Niles *et al.*, 2012
BG1805	2 μm, *URA3*, P_{GAL1}, C-terminal tandem affinity (TAP) tag vector	GE Healthcare
pJT4317	BG1805 Ypk1-TAP	GE Healthcare

TABLE 2: Plasmids used in this study.

Ergosterol level

Cells from samples (5 ml) of exponentially growing cultures of $Ysp2^{WT}$ (YFR495) and $Ysp2^{AAA}$ (YFR494-A) cells were collected by centrifugation and resuspended in 900 μl of methanol/water (2:1) with 1.5 μl of sterol-containing internal standard mix (SPLASH mix, Avanti Polar Lipids, Alabaster, AL). Chloroform (400 μl) and acid-washed glass beads (100 μl) were added, and samples were vortexed at 4°C for 10 min. Samples were then centrifuged for 10 min at 4°C at 15,000 × g. The organic phase (100 μl) was collected and dried under N_2. Lipid species in these samples were analyzed by liquid chromatography mass spectrometry, as described in detail in Keckesova *et al.* (2017). Ergosterol was detected in positive mode as the $(M+H-H_2O)+$ ion at *m/z* of 379.3367. Ergosterol peak areas were normalized to peak areas of the SPLASH internal standards to account for sample recovery and relative ergosterol content was then calculated.

ACKNOWLEDGMENTS

We thank Jasper Rine (University of California, Berkeley) for the gift of lovastatin, Ted Powers (University of California, Davis) for the gift of plasmids and anti-Ypk1 phospho-T662 antibodies, and Caroline A. Lewis (Metabolite Profiling Core Facility, MIT, Cambridge, MA) for mass spectrometry analysis of total cellular ergosterol content. This research was supported by Qatar National Research Fund Grant NPRP7-082-1-014 (to A.K.M.), by UK Biotechnology and Biological Sciences Research Council (BBSRC) Grant BB/P003818 (to T.P.L.), and by National Institutes of Health R01 Research Grant GM21841 (to J.T.).

REFERENCES

Alvaro CG, Aindow A, Thorner J (2016). Differential phosphorylation provides a switch to control how α-arrestin Rod1 down-regulates mating pheromone response in *Saccharomyces cerevisiae*. Genetics 203, 299–317.

Alvaro CG, O'Donnell AF, Prosser DC, Augustine AA, Goldman A, Brodsky JL, Cyert MS, Wendland B, Thorner J (2014). Specific α-arrestins negatively regulate *Saccharomyces cerevisiae* pheromone response by down-modulating the G-protein coupled receptor Ste2. Mol Cell Biol 34, 2660–2681.

Bardwell L, Cook JG, Zhu-Shimoni JX, Voora D, Thorner J (1998). Differential regulation of transcription: repression by unactivated mitogen-activated protein kinase Kss1 requires the Dig1 and Dig2 proteins. Proc Natl Acad Sci USA 95, 15400–15405.

Bari VK, Sharma S, Alfatah M, Mondal AK, Ganesan K (2015). Plasma membrane proteolipid-3 protein modulates amphotericin B resistance through sphingolipid biosynthetic pathway. Sci Rep 5, 9685.

Basson ME, Thorsness M, Rine J (1986). *Saccharomyces cerevisiae* contains two functional genes encoding 3-hydroxy-3-methylglutaryl-coenzyme A reductase. Proc Natl Acad Sci USA 83, 5563–5567.

Baum P, Thorner J, Honig L (1978). Identification of tubulin from the yeast *Saccharomyces cerevisiae*. Proc Natl Acad Sci USA 75, 4962–4966.

Berchtold D, Piccolis M, Chiaruttini N, Riezman I, Riezman H, Roux A, Walther TC, Loewith R (2012). Plasma membrane stress induces relocalization of Slm proteins and activation of TORC2 to promote sphingolipid synthesis. Nat Cell Biol 14, 542–547.

Carvalho M, Schwudke D, Sampaio JL, Palm W, Riezman I, Dey G, Gupta GD, Mayor S, Riezman H, Shevchenko A, *et al.* (2010). Survival strategies of a sterol auxotroph. Development 137, 3675–3685.
Chiapparino A, Maeda K, Turei D, Saez-Rodriguez J, Gavin AC (2016). The orchestra of lipid-transfer proteins at the crossroads between metabolism and signaling. Prog Lipid Res 61, 30–39.
da Silveira Dos Santos AX, Riezman I, Aguilera-Romero MA, David F, Piccolis M, Loewith R, Schaad O, Riezman H (2014). Systematic lipidomic analysis of yeast protein kinase and phosphatase mutants reveals novel insights into regulation of lipid homeostasis. Mol Biol Cell 25, 3234–3246.
Dittman JS, Menon AK (2017). Speed limits for nonvesicular intracellular sterol transport. Trends Biochem Sci 42, 90–97.
Dos Santos AG, Marquês JT, Carreira AC, Castro IR, Viana AS, Mingeot-Leclercq MP, de Almeida RFM, Silva LC (2017). The molecular mechanism of Nystatin action is dependent on the membrane biophysical properties and lipid composition. Phys Chem Chem Phys 15, 30078–30088.
Drin G, Moser von Filseck J, Čopič A (2016). New molecular mechanisms of inter-organelle lipid transport. Biochem Soc Trans 44, 486–492.
Gatta AT, Wong LH, Sere YY, Calderón-Noreña DM, Cockcroft S, Menon AK, Levine TP (2015). A new family of StART domain proteins at membrane contact sites has a role in ER-PM sterol transport. Elife 4, e07235.
Georgiev AG, Sullivan DP, Kersting MC, Dittman JS, Beh CT, Menon AK (2011). Osh proteins regulate membrane sterol organization but are not required for sterol movement between the ER and PM. Traffic 12, 1341–1355.
Guerreiro JF, Muir A, Ramachandran S, Thorner J, Sá-Correia I (2016). Sphingolipid biosynthesis upregulation by TOR complex 2-Ypk1 signaling during yeast adaptive response to acetic acid stress. Biochem J 473, 4311–4325.
Gupta SS, Ton VK, Beaudry V, Rulli S, Cunningham K, Rao R (2003). Antifungal activity of amiodarone is mediated by disruption of calcium homeostasis. J Biol Chem 278, 28831–28839.
Hampton RY, Rine J (1994). Regulated degradation of HMG-CoA reductase, an integral membrane protein of the endoplasmic reticulum, in yeast. J Cell Biol 125, 299–312.
Hannich JT, Umebayashi K, Riezman H (2011). Distribution and functions of sterols and sphingolipids. Cold Spring Harb Perspect Biol 3, a004762.
Hillenmeyer ME, Fung E, Wildenhain J, Pierce SE, Hoon S, Lee W, Proctor M, St Onge RP, Tyers M, Koller D, *et al.* (2008). The chemical genomic portrait of yeast: uncovering a phenotype for all genes. Science 320, 362–365.
Horenkamp FA, Valverde DP, Nunnari J, Reinisch KM (2018). Molecular basis for sterol transport by StART-like lipid transfer domains. EMBO J 37, e98002.
Jentsch JA, Kiburu I, Pandey K, Timme M, Ramlall T, Levkau B, Wu J, Eliezer D, Boudker O, Menon AK (2018). Structural basis of sterol binding and transport by a yeast StARkin domain. J Biol Chem 293, 5522–5531.
Jin H, McCaffery JM, Grote E (2008). Ergosterol promotes pheromone signaling and plasma membrane fusion in mating yeast. J Cell Biol 180, 813–826.
Jones EW (2002). Vacuolar proteases and proteolytic artifacts in *Saccharomyces cerevisiae*. Methods Enzymol 351, 127–150.
Kamiński DM (2014). Recent progress in the study of the interactions of amphotericin B with cholesterol and ergosterol in lipid environments. Eur Biophys J 43, 453–467.
Keckesova Z, Donaher JL, De Cock J, Freinkman E, Lingrell S, Bachovchin DA, Bierie B, Tischler V, Noske A, Okondo MC, *et al.* (2017). LACTB is a tumor suppressor that modulates lipid metabolism and cell state. Nature 543, 681–686.
Kentala H, Weber-Boyvat M, Olkkonen VM (2016). OSBP-related protein family: mediators of lipid transport and signaling at membrane contact sites. Int Rev Cell Mol Biol 321, 299–340.
Kinoshita E, Kinoshita-Kikuta E, Koike T (2015). Advances in Phos-tag-based methodologies for separation and detection of the phosphoproteome. Biochim Biophys Acta 1854, 601–608.
Klug L, Daum G (2014). Yeast lipid metabolism at a glance. FEMS Yeast Res 14, 369–388.
Kuranda K, François J, Palamarczyk G (2010). The isoprenoid pathway and transcriptional response to its inhibitors in the yeast *Saccharomyces cerevisiae*. FEMS Yeast Res 10, 14–27.
Lavigne P, Najmanivich R, Lehoux JG (2010). Mammalian StAR-related lipid transfer (START) domains with specificity for cholesterol: structural conservation and mechanism of reversible binding. Subcell Biochem 51, 425–437.
Lee YJ, Jeschke GR, Roelants FM, Thorner J, Turk BE (2012). Reciprocal phosphorylation of yeast glycerol-3-phosphate dehydrogenases in adaptation to distinct types of stress. Mol Cell Biol 32, 4705–4717.
Li X, Gianoulis TA, Yip KY, Gerstein M, Snyder M (2010). Extensive in vivo metabolite-protein interactions revealed by large-scale systematic analyses. Cell 143, 639–650.
Li Y, Prinz WA (2004). ATP-binding cassette (ABC) transporters mediate nonvesicular, raft-modulated sterol movement from the plasma membrane to the endoplasmic reticulum. J Biol Chem 279, 45226–45234.
Lingwood D, Simons K (2010). Lipid rafts as a membrane-organizing principle. Science 327, 46–50.
Maxfield FR, Iaea DB, Pipalia NH (2016). Role of STARD4 and NPC1 in intracellular sterol transport. Biochem Cell Biol 94, 499–506.
Muir A, Ramachandran S, Roelants FM, Timmons G, Thorner J (2014). TORC2-dependent protein kinase Ypk1 phosphorylates ceramide synthase to stimulate synthesis of complex sphingolipids. Elife 3, e03779.
Muir A, Roelants FM, Timmons G, Leskoske KL, Thorner J (2015). Down-regulation of TORC2-Ypk1 signaling promotes MAPK-independent survival under hyperosmotic stress. Elife 4, e09336.
Murley A, Sarsam RD, Toulmay A, Yamada J, Prinz WA, Nunnari J (2015). Ltc1 is an ER-localized sterol transporter and a component of ER-mitochondria and ER-vacuole contacts. J Cell Biol 209, 539–548.
Murley A, Yamada J, Niles BJ, Toulmay A, Prinz WA, Powers T, Nunnari J (2017). Sterol transporters at membrane contact sites regulate TORC1 and TORC2 signaling. J Cell Biol 216, 2679–2689.
Niles BJ, Mogri H, Hill A, Vlahakis A, Powers T (2012). Plasma membrane recruitment and activation of the AGC kinase Ypk1 is mediated by target of rapamycin complex 2 (TORC2) and its effector proteins Slm1 and Slm2. Proc Natl Acad Sci USA 109, 1536–1541.
Raychaudhuri S, Prinz WA (2010). The diverse functions of oxysterol-binding proteins. Annu Rev Cell Dev Biol 26, 157–177.
Rispal D, Eltschinger S, Stahl M, Vaga S, Bodenmiller B, Abraham Y, Filipuzzi I, Movva NR, Aebersold R, Helliwell SB, Loewith R (2015). Target of Rapamycin Complex 2 regulates actin polarization and endocytosis via multiple pathways. J Biol Chem 290, 14963–14978.
Roelants FM, Baltz AG, Trott AE, Fereres S, Thorner J (2010). A protein kinase network regulates the function of aminophospholipid flippases. Proc Natl Acad Sci USA 107, 34–39.
Roelants FM, Breslow DK, Muir A, Weissman JS, Thorner J (2011). Protein kinase Ypk1 phosphorylates regulatory proteins Orm1 and Orm2 to control sphingolipid homeostasis in *Saccharomyces cerevisiae*. Proc Natl Acad Sci USA 108, 19222–19227.
Roelants FM, Leskoske KL, Pedersen RT, Muir A, Liu JM, Finnigan GC, Thorner J (2017). TOR complex 2-regulated protein kinase Fpk1 stimulates endocytosis via inhibition of Ark1/Prk1-related protein kinase Akl1 in *Saccharomyces cerevisiae*. Mol Cell Biol 37, e00627–16.
Sambrook J, Fritsh EF, Maniatis T (1989). Molecular Cloning: A Laboratory Manual, Cold Spring Harbor, NY: Cold Spring Harbor Laboratory Press.
Sharma S, Alfatah M, Bari VK, Rawal Y, Paul S, Ganesan K (2014). Sphingolipid biosynthetic pathway genes *FEN1* and *SUR4* modulate amphotericin B resistance. Antimicrob Agents Chemother 58, 2409–2414.
Sherman F, Fink GR, Hicks JB (1986). Laboratory Course Manual for Methods in Yeast Genetics, Cold Spring Harbor, NY: Cold Spring Harbor Laboratory Press.
Sikorski RS, Hieter P (1989). A system of shuttle vectors and yeast host strains designed for efficient manipulation of DNA in *Saccharomyces cerevisiae*. Genetics 122, 19–27.
Sokolov S, Knorre D, Smirnova E, Markova O, Pozniakovsky A, Skulachev V, Severin F (2006). Ysp2 mediates death of yeast induced by amiodarone or intracellular acidification. Biochim Biophys Acta 1757, 1366–1370.
Tong J, Manik MK, Im YJ (2018). Structural basis of sterol recognition and nonvesicular transport by lipid transfer proteins anchored at membrane contact sites. Proc Natl Acad Sci USA 115, E856–E865.
Tsujishita Y, Hurley JH (2000). Structure and lipid transport mechanism of a StAR-related domain. Nat Struct Biol 7, 408–414.
van Meer G, Voelker DR, Feigenson GW (2008). Membrane lipids: where they are and how they behave. Nat Rev Mol Cell Biol 9, 112–124.
Wong LH, Levine TP (2016). Lipid transfer proteins do their thing anchored at membrane contact sites … but what is their thing? Biochem Soc Trans 44, 517–527.
Yang ST, Kreutzberger AJ, Lee J, Kiessling V, Tamm LK (2016). The role of cholesterol in membrane fusion. Chem Phys Lipids 199, 136–143.